COMPACTION BEHAVIOR OF FABRIC PREFORMS IN RESIN TRANSFER MOLDING PROCESS

Baoxing Chen [1], Eric J. Lang [2], and Tsu-Wei Chou [1]

[1] *Center for Composite Materials and Department of Mechanical Engineering*
University of Delaware, Newark, DE 19716, U.S.A
[2] *The Why Not Corp., 743 W. Sparrow Rd., Springfield, OH 45502, U.S.A*

SUMMARY: The compaction behavior of fabric preforms in resin transfer molding (RTM) process has been investigated. Compaction experiments were carried out for three types of preforms, continuous strand mat, plain woven fabric, and a unidirectional knitted material. Five main factors affecting the properties of finished parts in RTM process are identified first, and their influences on the compaction behavior of the preforms are then discussed. The theoretical part of this paper focuses on improving the simplified 3D micro-mechanical model proposed recently by the authors. Analytical expressions for the relations among the fiber volume fraction, the applied compressive force, and the preform thickness reduction, have been established using the improved model, which is suitable for any type of pressure distribution at contacting regions between adjacent fabrics. As examples, closed from solutions have been obtained for uniform, linear, and sinusoidal pressure distributions. The improved model and the simplified model are compared and discussed.

KEYWORDS: fabrics, resin transfer molding, woven composites, compaction.

INTRODUCTION

Fabric composite materials based upon 2D and 3D textile preforms have received considerable attention in recent years. The merits of fabric composites include ease of fabrication, cost-effectiveness, and enhanced properties in the thickness direction. Among various composite-molding techniques, RTM is of very high potential. While the preforming process, such as weaving, knitting, braiding and stitching, places the fiber into a skeleton of the actual part, the final fiber microstructure depends to a certain extent on the compaction of the preform to the designed thickness. Although a number of factors in RTM process affect the properties of the finished composites, the compaction of the preform during tool closure is of major importance.

A literature review of the compaction behavior of textile reinforcements in composite manufacturing has recently been conducted by Robitail and Gauvin [1]. The experimental work by Matsudaira and Qin [2], Pearce and Summerscale [3], Sauders, Lekakou and Bader [4], provided enlightening insights into the compaction of plain-woven fabric preforms. A

number of experimental works on the compaction behavior can be found in the open literature. However, few investigations have focused on modeling the preform compaction behavior theoretically, in spite of the fact that various regression relations for fabric preforms have been proposed based upon experimental results.

Recently the authors [5, 6] have conducted a theoretical study of the compaction behavior of plain-weave fabric preforms. Simplified 3D micro-mechanical models for both single-layer and multiple-layer fabrics were developed for predicting the compaction behavior. This paper first presents our compaction experiments for three types of preforms, i.e., continuous strand mat, plain woven fabric, and a unidirectional knitted material. Then, five main factors affecting the preform compaction in RTM process are identified. The theoretical part of this paper focuses on improving the simplified 3D micro-mechanical model of a single-layer plain-weave fabric. The improved model is suitable for any type of pressure distribution between adjacent fabric layers and is compared with the simplified model.

COMPACTION EXPERIMENTS

Outline of the Experiments

Fiberglass preform thickness as a function of applied pressure was measured for three different preform materials – continuous strand mat, plain woven fabric, and a unidirectional knitted material. These materials each have a unique compaction response due in part to their differing microstructures. Compaction experiments were run on single 305mm by 305mm (12"x12") layers as well as stacks of 10 and 25 layers of each of these materials. The compaction experiments were performed in a hydraulic press using two steel plates approximately 457mm (18") on a side and 38mm (1.5") thick. The plates had been specially ground to a flat surface. The distance between the steel plates was measured as a function of the applied compressive force. The average thickness per layer versus compaction pressure was then calculated for each combination of preform material and number of layers of fabric and is shown in Fig. 1.

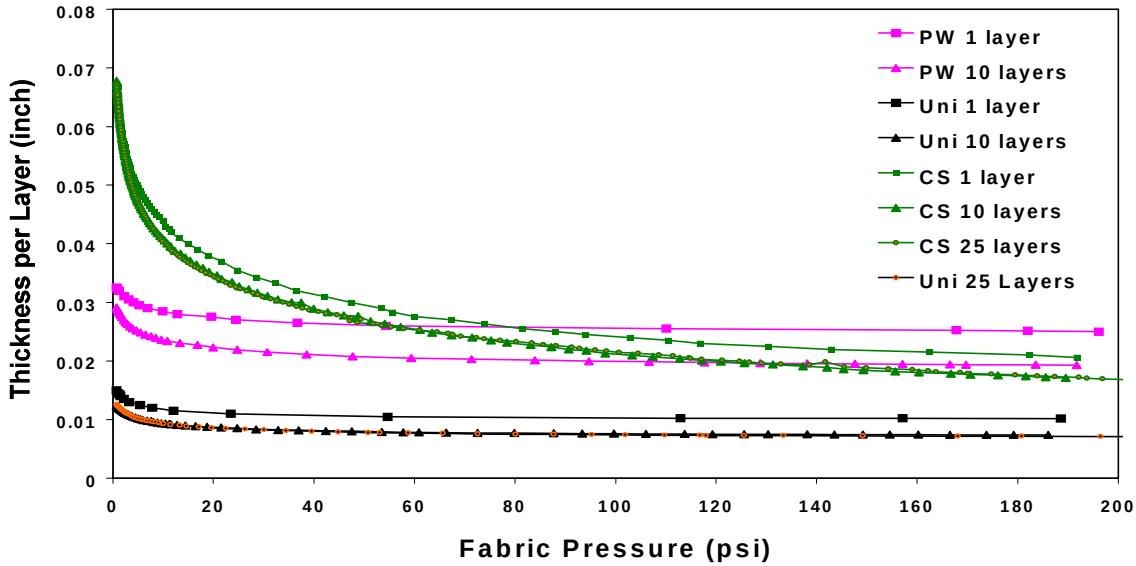

Fig. 1: Thickness per layer versus fabric pressure

One observation is that for a given compaction pressure and preform material, the thickness per layer for a stack of 10 or 25 layers of material is less than the thickness of a single layer. The reason for this is the "nesting" of the "hills" and "valleys" of adjacent layers. The thickness per layer for 10 layers and 25 layers are very similar which suggests that the nesting effect reached a steady state by 10 layers. Obviously, nesting exists even at the beginning of compression for plain woven and unidirectional materials, but not for continuous strand mat.

Micro-structural Analysis

Observing the deformation of fibers and fiber bundles during compaction without disturbing the fibers and fiber bundles themselves presents many challenges. Therefore, some composite plates were made in which the preforms were in various states of compaction. Samples were cut from each plate, edge polished and photographed under a microscope. In the case of the plain-woven material and the unidirectional material, photographs were made of both the warp view and the weft view. In warp view, warp yarns are seen in cross-section whereas in weft view, weft yarns are shown in cross-section. In the case of the continuous strand mat there is no distinction between warp or weft views since it is assumed that the material is transversely isotropic.

Table 1 gives the details on the composite plates. The number of layers of a given preform material was chosen so that the weight of fiberglass per unit area will be roughly the same for all three preform material types. After the composite plate cured, the thickness of the plate was measured. The applied fabric pressure was determined by calculating the thickness per layer of the composite plate and then using the data from the compaction experiments to determine the pressure acting on the preform. The compacted preforms were infiltrated using a vacuum to draw the resin through the compacted preform from one edge of the preform to the other in a one-dimensional flow pattern. The mass of resin entering the part as a function of time was recorded.

Table 1: Outline of compaction experiments

Fabric Types	Fabric Density kg/sheet/m^2 (gm/sheet/ft^2)	Number of Layers	Composite Thickness mm(inches)	Fabric Pressure mPa (psi)	Fiber Volume Fraction	Infiltration Time (minutes)
Plain weave	0.818(76)	10	10.16(0.4")	0.000(0.0)	29%	2
Plain weave	0.818(76)	10	7.62(0.3")	0.005(0.7)	38%	8
Plain weave	0.818(76)	10	6.35(0.25")	0.036(5.2)	46%	11
Plain weave	0.818(76)	10	4.70(0.185")	1.517(220)	62%	14
Unidirectional	0.315(29.3)	25	10.16(0.4")	0.000(0.0)	28%	2.5
Unidirectional	0.315(29.3)	25	6.99(0.275")	0.019(2.8)	40%	7.5
Unidirectional	0.315(29.3)	25	5.72(0.225")	0.099(14.4)	49%	10
Continuous strand	0.307(28.5)	25	12.70(0.5")	0.820(119)	22%	11.5
Continuous strand	0.307(28.5)	25	10.16(0.4")	2.344(340)	27%	23

PARAMETERS AFFECTING THE PREFORM COMPACTION

From compaction experiments, five main factors are identified as the sources of preform compaction. The influences of these factors on the compaction of different preforms are summarized in Table 2.

Table 2: Factors affecting the compaction behavior of preforms

Main Factors	Preforms		
	Random mat	Non-woven	Woven
Yarn cross-section deformation	**	**	**
Yarn flattening	*		**
Yarn bending deformation	*	*	*
Void condensation	**	*	*
Nesting		*	**

** Strong effect * Less strong effect

Table 2 indicates that *yarn cross-section deformation* has a strong effect on the compaction of all three types of preforms, while *yarn bending deformation* has a less strong influence on the compaction of these fabrics. This can be seen clearly from the image-processed sections of the compressed specimens to various degrees of compaction. Because of the length limit of this paper, the micrographs of our experiments are not reported here. Interested readers can refer to the similar pictures reported in Ref. 4. *Void condensation* is a more important factor for describing the compaction behavior of random mats than for non-woven and woven fabrics. *Nesting* is a dominant factor for woven fabrics but not for random mats. Nesting has a week effect on the behavior of non-woven fabrics. *Yarn flattening* has almost no contribution to the compaction of non-woven fabrics, while it affects the compaction behavior of woven fabrics as well as random mats.

COMPACTION MODELS OF PLAIN-WEAVE FABRIC PREFORMS

Summary of Previous Analytical Work

In previous papers [5,6], micro-mechanical models for predicting the compaction behavior of a single layer and multi-layers of plain-weave fibrous preform in RTM processes were developed on the basis of the following assumptions: (a) The unit cell repeats in the plane of the fabric, which is infinite in extent. (b) The yarn is treated as a transversely isotropic solid, i.e., the fibers in the yarn are highly compacted. (c) The external compressive force is applied uniformly on the fabric preform. (d) The elastic deformation of the fabric takes place only in its thickness direction, i.e., neglecting its in-plane deformation. (e) No voids and gaps exist between the yarns. (f) During the compaction process, the yarn shape deforms, but the yarn cross-sectional area remains unchanged, i.e., constant yarn packing fraction.

The analysis in Ref. 5, focused on the *unit cell* of an orthogonal plain-weave fibrous preform, which is composed of two sets of mutually orthogonal yarns. A 3D model of the unit cell was developed and used to predict the compressive behavior of yarns. One quarter of this unit cell model of the fabric geometric configuration at the initial stage of bending deformation is shown in Fig. 2. Analytical expressions for relations among the fiber volume fraction, the applied compressive force and the preform thickness reduction have been established. A prediction of the limiting fiber volume fraction is also obtained.

Based upon the proposed compaction models and beam theory in the mechanics of materials, Ref. 6 presented the analytical results for the nesting and elastic deformation during the compaction of multi-layer woven-fabric preforms. Analytical expressions for relations among the fiber volume fraction, the applied compressive force, and the preform thickness reduction

have been established for non-nesting and maximum nesting cases. For the general nesting cases, an empirical relation between the compressive force and the thickness reduction is proposed. The models and results of these studies also have significant implication in the understanding of preform permeability in RTM processes. The permeability calculation [7] has been carried out recently by the authors based upon the micro-mechanical models.

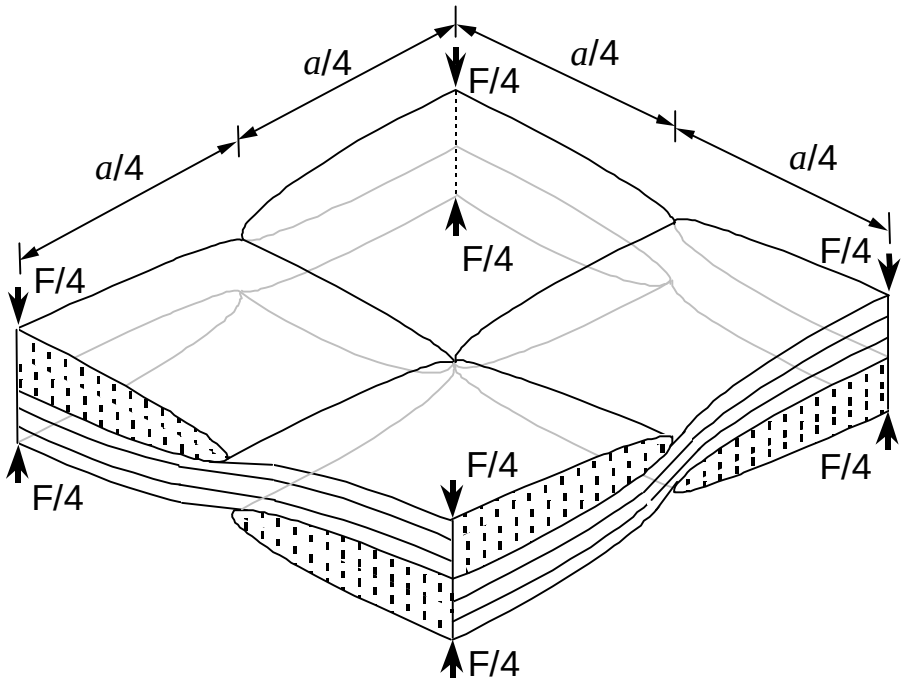

Fig. 2: One quarter of 3D unit cell of a plain-weave fibrous preform

Description of Compaction Behavior

In Ref. 5, the elastic deformation of a single-layer woven fabric was described as follows. At first, the compressive force acts at the highest (or lowest) points of the upper (or lower) surface of the fabric as shown in Fig. 2. As the compressive force increases, elastic deformation of the fabric extends, and the thickness of the fabric preform decreases while the fiber volume fraction increases. Also, the external force distributes over a contacting area. This contacting area expands as the external force increases. When the force reaches a certain value, the fabric cannot be further compressed.

In Ref. 6, the nesting between two adjacent fabric layers was predicted first and then the compaction owing to tool closure was modeled. The compaction was described as follows, for the bottom fabric layer of a two-layer plain-weave preform, for example. The compressive force acts at the lowest points of the bottom surface of the bottom fabric layer, as well as at the contacting points between the upper fabric and lower fabric. As the externally applied compressive force increases, elastic deformation of the fabric extends, and the thickness of the fabric preform decreases while the fiber volume fraction increases. Also, the external force distributes over a contacting area. The contacting area expands as the external force increases. It was assumed that the yarn cross-sectional area remains unchanged, even though the shape of the yarn cross-section changes with increasing compressive forces. When the applied force reaches a limiting value, the fabric cannot be further compressed and the yarn cross-section

approaches to a rectangle as shown in Fig. 5 of Ref. 5, which represents the well-known mosaic model for woven-fabric composites proposed by Ishikawa and Chou [8, 9]. Similarly, the compaction of the top layer of the two-layer woven fabric preform could be described. For multi-layer woven fabrics, the compaction of the top layer and the bottom layer is the same as those described above, but the compaction of the internal layers between the top and bottom layers were different from those of the top and bottom layers because of the nesting effects.

Improved Micro-mechanical Models

In Ref. 5, a micro-mechanical model (Fig. 3) was developed for predicting the compaction behavior in which the concentrated forces were used for simplicity. Obviously, the pressure distribution was not considered in this simplified model. For a more realistic compaction model, it is necessary to consider the pressure distribution. To better model the pressure between layers during compaction, we proposed three types of pressure distribution to improve the simplified model. These include the uniform pressure distribution model (Fig. 4), the linear pressure distribution model (Fig. 5), and the sinusoidal pressure distribution model (Fig. 6). For all three models, the resultant compression forces are the same as those shown in Fig. 3 for the simplified model.

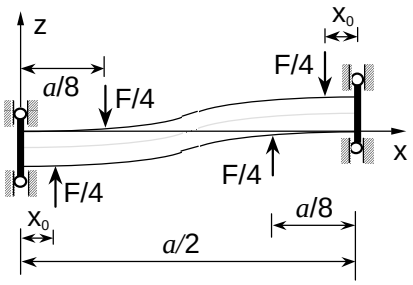

Fig. 3: Simplified micro-mechanical model with concentrated compressive forces

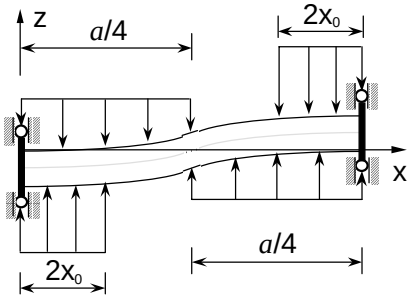

Fig. 4: Uniform pressure distribution model

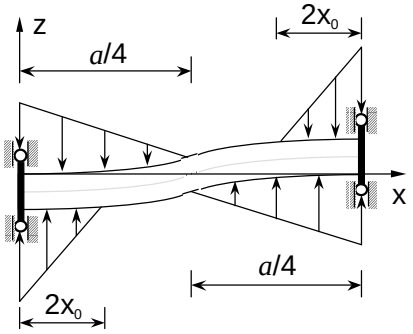

Fig. 5: Linear pressure distribution model

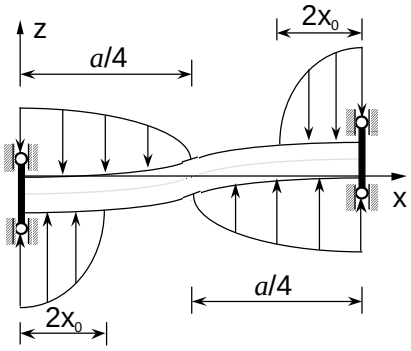

Fig. 6: Sinusoidal pressure distribution model

Using an analysis [5] similar to that for the simplified model (Fig. 3), closed form solutions of the relation between the applied compressive force F and the thickness reduction r_z can readily be obtained as follows for the three improved models of Figs. 4-6, respectively.

For uniform pressure distribution,

$$F = \frac{16E(\pi-2)^2[4(\pi-2)h_y + \pi r_z]r_z(2h_y - r_z)^5}{3\pi a^2[8r_z^3 - 16(\pi-2)(2h_y - r_z)r_z^2 + 3(\pi-2)^3(2h_y - r_z)^3]} \tag{1}$$

For linear pressure distribution,

$$F = \frac{10E(\pi-2)^2[4(\pi-2)h_y + \pi r_z]r_z(2h_y - r_z)^5}{3\pi a^2[2r_z^3 - 5(\pi-2)(2h_y - r_z)r_z^2 + (\pi-2)^3(2h_y - r_z)^3]} \tag{2}$$

For sinusoidal pressure distribution,

$$F = \frac{2E\pi^2(\pi-2)^2[4(\pi-2)h_y + \pi r_z]r_z(2h_y - r_z)^5}{3a^2[4(\pi^3 - 24\pi + 48)r_z^3 - 6\pi(\pi^2 - 8)(\pi-2)(2h_y - r_z)r_z^2 + (\pi^3 - 24)(\pi-2)^3(2h_y - r_z)^3]} \tag{3}$$

In above equations, a represents the length and width of the unit cell, $2h_y$ is the thickness of the fabric, E stands for the axial Young's modulus of the yarn, and $0 \le r_z \le r_z^{\max}$. The maximum thickness reduction $r_z^{\max}$ is expressed as

$$r_z^{\max} = 2(1 - 2/\pi)h_y . \tag{4}$$

Solving Eqs. (1)-(3), respectively, the thickness reduction can be expressed in terms of the externally applied compressive force:

$$r_z = g(F) . \tag{5}$$

It should be noted that it is not difficult to obtaine function $g(F)$ numerically, in spite of the fact that it cannot be solved explicitly from Eqs. (1)-(3). Having obtained the thickness reduction expression, the fiber volume fraction V_f can readily be expressed in terms of the applied compressive force as follows:

$$V_f = \frac{2}{\pi[1 - g(F)/(2h_y)]}V_a , \tag{6}$$

where V_a represents the yarn packing fraction [5].

Parametric Results of the Improved Models

Figure 7 shows the relation of non-dimensional compressive force versus non-dimensional thickness reduction for the three improved models developed in this paper. The results from the simplified model are shown in Fig. 7 in dashed line for comparison. The relations of the

non-dimensional compressive force versus non-dimensional thickness are given in Fig. 8. The curves of non-dimensional fiber volume fraction versus non-dimensional compressive force are plotted in Fig. 9.

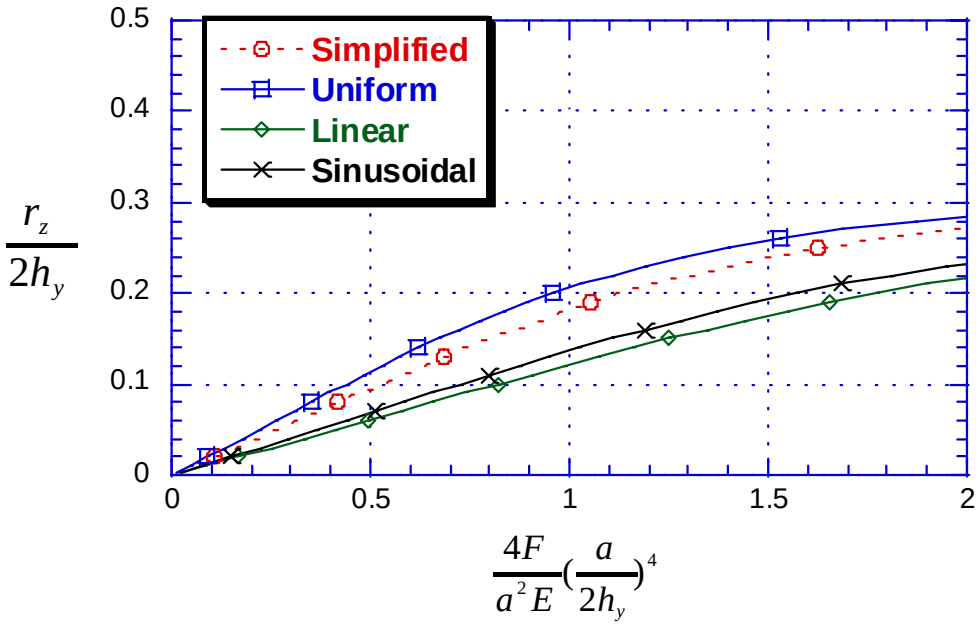

Fig. 7: Non-dimensional compressive force versus non-dimensional thickness reduction

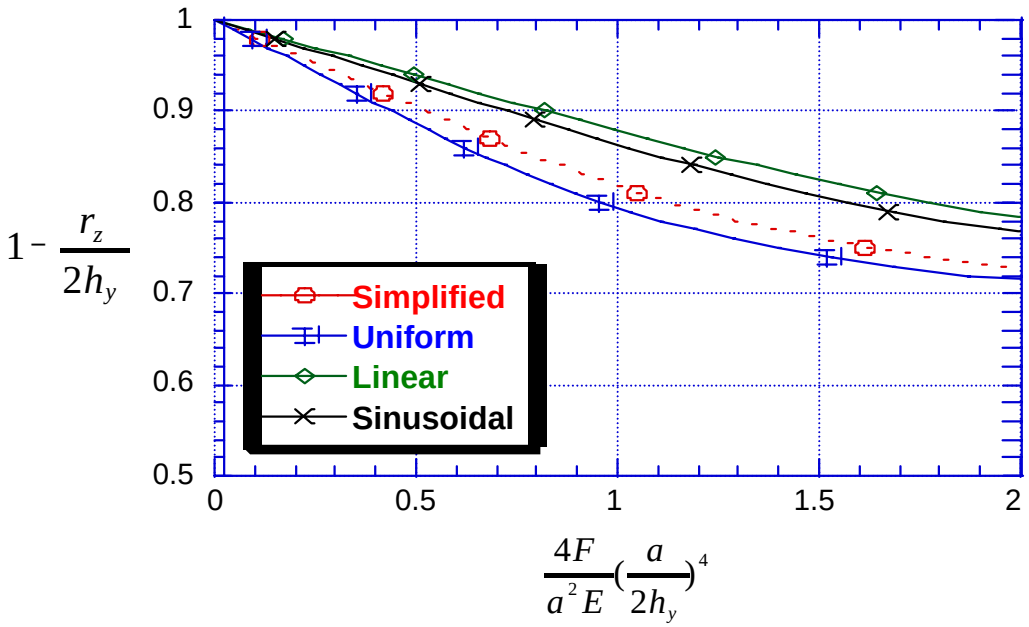

Fig. 8: Non-dimensional compressive force versus non-dimensional thickness

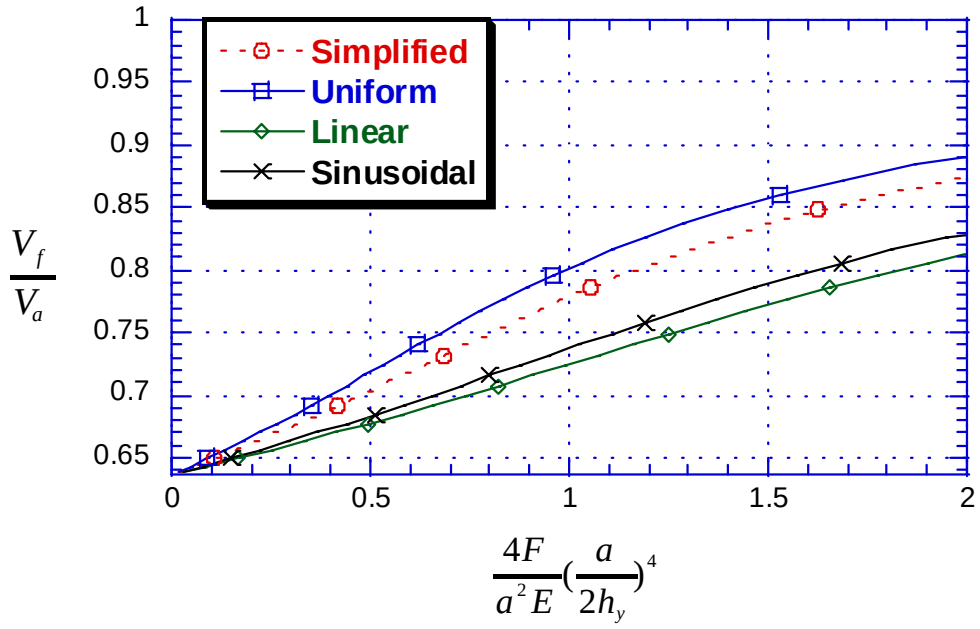

Fig. 9: Non-dimensional fiber volume fraction versus non-dimensional compressive force

CONCLUDING REMARKS

1. Compaction experiments were carried out for three types of preforms, i.e., continuous strand mat, plain woven fabric, and a unidirectional knitted material.
2. Five main factors affecting the compaction behavior of fabric preforms in RTM process have been identified.
3. Improved compaction models for a single-layer plain-woven fabric have been developed based upon the assumed contacting pressure distributions.
4. Analytical expressions for the relations among the fiber volume fraction, the applied force, and the preform thickness reduction, have been obtained using improved models.
5. More complicated compaction pressure distributions can also be modeled using a procedure similar to that developed in this paper.
6. Further research is needed for validating the theoretical modeling results by experiments.

ACKNOWLEDGMENTS

This work was supported by the Advanced Materials Intelligent Processing Center of the Office of Naval Research at the University of Delaware under contract number N00014-97-C-0415. James J. Kelly is the Program Manager.

REFERENCES

1. Robitaille, F. and Gauvin R., "Compaction of textile reinforcements for composites manufacturing I: review of experimental results". *Polymer Composites*, Vol. 19, No. 2, 1998, pp. 198-216.

2. Matsudaira, M. and Qin, H., "Features and mechanical properties of a fabric's compressional property", *Journal of Textile Institute*, Vol. 86, 1995, pp. 476-486.

3. Pearce N. and Summerscales, J., "The compressibility of a reinforcement fabric", *Composites Manufacturing*, Vol. 6, 1995, pp. 15-21.

4. Saunders, R.A., Lekakou, C. and Bader, M.G., "Compression and microstructure of fiber plain woven cloths in the processing of polymer composites", *Composites Part A*, Vol. 29A, 1998, pp. 443-454.

5. Chen, B. and Chou, T.-W., "Compaction of woven fabric preforms in liquid composite molding processes: single-layer deformation", *Composites Science and Technology*, Vol. 59, in press, 1999

6. Chen, B. and Chou, T.-W., "Compaction of woven fabric preforms in liquid composite molding processes: nesting and multi-layer deformation", *Composites Science and Technology*, submitted for publication, 1999.

7. Sozer, E.M., Chen, B., Graham, P.J., Chou, T.-W., and Advani, S.G., "Characterization and prediction of compaction force and preform permeability of woven fabrics during the resin transfer molding process", to be presented at *The Fifth International Conference on Flow Processes in Composite Materials*, Plymouth, U.K., July 12-14, 1999.

8. Ishikawa, T. and Chou, T.-W., "Stiffness and strength behavior of woven fabric composites", *Journal of Materials Science*, Vol. 17, 1982, pp. 3211-3220.

9. Chou, T.-W., *Microstructural Design of Fiber Composites*, Cambridge University Press, Cambridge, 1992.